Biology of Reproduction, 2019, 100(6), 1461–1472
doi:10.1093/biolre/ioz052
Research Article
Advance Access Publication Date: 2 April 2019

OXFORD

Research Article

The perforatorium and postacrosomal sheath of rat spermatozoa share common developmental origins and protein constituents†

Nicole Protopapas [1,‡], Lauren E. Hamilton [1,‡], Ruben Warkentin [1], Wei Xu[1], Peter Sutovsky [2,3] and Richard Oko [1,*]

[1]Department of Biomedical and Molecular Sciences, Queen's University, Kingston, Ontario, Canada; [2]Division of Animal Sciences, College of Agriculture, Food and Natural Resources, University of Missouri, Colombia, Missouri, USA and [3]Department of Obstetrics, Gynecology and Women's Health, School of Medicine, University of Missouri, Colombia, Missouri, USA

*__Correspondence:__ Department of Biomedical and Molecular Sciences, Queen's University, Botterell Hall, 18 Stuart Street, Kingston, ON K7L 3N6, Canada. E-mail: ro3@queensu.ca

†__Grant Support:__ This work was supported by the Canadian Institute of Health Research (84440) and the Natural Science and Engineering Research Council of Canada (RGPIN/05305) to RO, along with the Agriculture and Food Research Initiative Competitive Grant no. 2015-67015-23231 from the USDA National Institute of Food and Agriculture and seed funding from the Food for the 21st Century Program of the University of Missouri to PS.
__Conference presentation__: Presented in part at the 51st annual meeting of the Society for the Study of Reproduction, 10–13 July, 2018, New Orleans, Louisiana.
‡These authors contributed equally to this work.

Received 14 December 2018; Revised 1 March 2019; Accepted 29 March 2019

Abstract

The perinuclear theca (PT) is a cytosolic protein capsule that surrounds the nucleus of eutherian spermatozoa. Compositionally, it is divided into two regions: the subacrosomal layer (SAL) and the postacrosomal sheath (PAS). In falciform spermatozoa, a third region of the PT emerges that extends beyond the nuclear apex called the perforatorium. The formation of the SAL and PAS differs, with the former assembling early in spermiogenesis concomitant with acrosome formation, and the latter dependent on manchette descent during spermatid elongation. The perforatorium also forms during the elongation phase of spermiogenesis, suggesting that like the PAS, its assembly is facilitated by the manchette. The temporal similarity in biogenesis between the PAS and perforatorium led us to compare their molecular composition using cell fractionation and immunodetection techniques. Although the perforatorium is predominantly composed of its endemic protein FABP9/PERF15, immunolocalization indicates that it also shares proteins with the PAS. These include WBP2NL/PAWP, WBP2, GSTO2, and core histones, which have been implicated in early fertilization and zygotic events. The compositional homogeny between the PAS and perforatorium supports our observation that their development is linked. Immunocytochemistry indicates that both PAS and perforatorial biogenesis depend on the transport and deposition of cytosolic proteins by the microtubular manchette. Proteins translocated from the manchette pass ventrally along the spermatid head into the apical perforatorial space prior to PAS deposition in the wake of manchette descent. Our findings demonstrate that the perforatorium and PAS share a mechanism of developmental assembly and thereby contain common proteins that facilitate fertilization.

Summary Sentence

The perforatorium is a distinct region of the perinuclear theca of falciform spermatozoa whose assembly during spermiogenesis is temporally and mechanistically linked to the postacrosomal sheath, resulting in many proteins being shared between these regions of the perinuclear theca.

Key words: gamete biology, spermiogenesis, spermatozoa, microtubular manchette, perinuclear theca, postacrosomal sheath, perforatorium, murids.

Introduction

The highly specialized nature of the mammalian spermatozoon is tribute to its dramatic transformation during the haploid phase of germ cell differentiation termed spermiogenesis. During this time, a series of cellular, molecular, and morphological changes transform a round spermatid into an elongated spermatozoon with a highly condensed nucleus and a collection of specialized accessory structures, including the acrosome and the perinuclear theca (PT) of the sperm head. Despite differences in morphology, the basic structural organization of the spermatozoon head is similar amongst eutherian mammals, with the nucleus and acrosome occupying much of the volume of the sperm head, and the remaining space filled by the PT.

The PT is the major cytoskeletal-like element of the sperm head that forms a dense layer of cytosolic material encapsulating the nucleus, except in the distal region of the perifossal zone where the tail implants. It is mostly a nonionic, detergent-resistant protein layer whose constituents have been implicated in several important functions during both spermiogenesis and fertilization [1–3].

Morphological and compositional analyses have divided the PT of spatulate spermatozoa into two structurally continuous but functionally distinct regions: the subacrosomal layer (SAL) and the postacrosomal sheath (PAS) (Figure 1A) [4, 5]. The proteins comprising the SAL are found apically in the sperm head between the inner acrosomal membrane and nuclear envelope. External to the acrosome in the equatorial segment region, the PT is enclosed by the outer acrosomal membrane and the plasmalemma, in an area referred to as the outer periacrosomal layer (OPL) [6]. The OPL is considered as a segment of the SAL due to its proteinaceous resemblance and similar assembly process [7–9]. The PT continues to extend caudally beyond the acrosome to form the PAS. The PAS encapsulates the base of the sperm nucleus where the acrosome is no longer present to occupy the area between the plasmalemma and nuclear envelope. Despite the compositional uniqueness of the SAL and PAS, structural continuity is maintained within the PT [4, 10].

Falciform spermatozoa, as seen in most murids such as laboratory mice and rats, present an additional component to the PT called the perforatorium (Figure 1B). The perforatorium extends beyond the apical aspect of the nucleus in the shape of a curved triangular rod, creating the characteristic hook-like appearance of most murid spermatozoa. The nucleus projects into the perforatorium centrally, giving rise to three interconnected perforatorial prongs (one dorsal, two ventral) to which the protruding triangular structure is anchored (see apical cross-sections, Figure 1B). The acrosome, along with the tightly adherent SAL, forms a triangular crest over the dorsal and lateral edges of the perforatorium, leaving the ventral surface void of acrosomal material, except for the displaced head cap segment (Figure 1B).

In addition to the apical perforatorium, many murid spermatozoa contain another cytoskeletal protrusion on the ventral concave surface of the sperm head called the ventral spur. The ventral spur is a modest thickening of the PT, compositionally organized into two layers: an inner layer of perforatorial material and an outer layer continuous with the PAS (Figure 1B) [6, 11, 12]. The compositional similarity between the perforatorium and inner ventral spur suggests these two structures are continuous with one another along the ventral concave surface of the sperm head. The murid family of rodents also includes species with a more highly complex head structure, including the hydromyine rodents of Australia, which contain two further ventral cytoskeletal projections in addition to the apical perforatorial hook [13–16].

The compositional uniqueness between the regions of the PT is akin to their differences in formation during spermiogenesis (Figure 2). The assembly of the SAL occurs early in spermiogenesis concomitant with the development of the nascent acrosome. Cytosolic SAL proteins coat the periphery of the acrosomic granule of early round spermatids prior to its attachment to the nuclear envelope. As the acrosomic system expands over the apical aspect of the spermatid nucleus, the SAL continues to develop synchronously between the inner acrosomal membrane and the nuclear envelope [5, 9, 17]. SAL proteins coating the outer acrosomal membrane disappear concomitantly with spermatid elongation, except along the equatorial segment where the OPL is demarcated. Taken together, the proteins of the SAL have been functionally implicated in acrosome assembly, including acrosome vesicle transport and nuclear attachment and expansion [1, 8, 9, 17].

As spermiogenesis continues into nuclear elongation and condensation, the PAS of the PT is formed (Figure 2). The elongation phase of spermiogenesis is characterized by the caudal manchette, a transient microtubular structure that encircles the base of the spermatid nucleus [18]. Analogous to the dependence of SAL formation on the developing acrosome, the descent of the manchette is deemed a requirement for PAS assembly [1, 17, 19–22]. At the onset of nuclear elongation, manchette microtubules extend caudally from the nuclear ring to the distal cytoplasmic lobe, creating a girdle-like structure that encapsulates the spermatid head below the acrosome. Proteins synthesized in the cytoplasmic lobe appear to be stored and transported up the microtubular manchette to the spermatid head in a process termed intramanchette transport [23]. Microtubule motor proteins, such as kinesins and dyneins, localized to the manchette, support its proposed role in protein transport [23, 24]. As the manchette migrates distally at the completion of spermatid elongation, proteins residing on the manchette are deposited in the space once occupied by the microtubules, thereby forming the PAS of the PT [1, 17, 19–22]. In rat, the descent of the manchette occurs between steps 15 and 16 of spermiogenesis, after which time the manchette begins to deteriorate in the cytoplasmic lobe. Previous studies on resident PAS proteins have provided evidence that supports this narrative of biogenesis, including WBP2NL/PAWP, the core histones, and GSTO2 [21, 22, 25]. In contrast to the SAL, proteins of the PAS have been functionally implicated in early fertilization events such as oocyte activation and pronuclear formation [1, 2, 25–29].

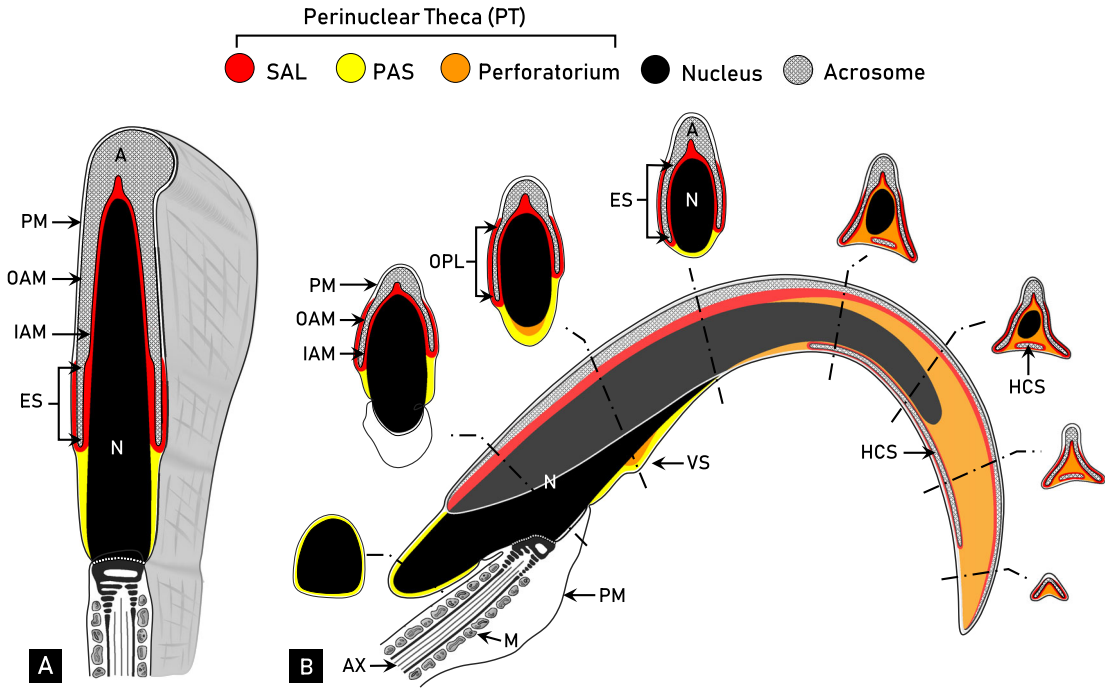

Figure 1. Comparative diagrammatic representations of a mid-sagittal section of spatulate (A, bovine) and falciform (B, rat) spermatozoa. The regional distinctions of the perinuclear theca (PT) of rat spermatozoa depicted in this figure, notably the characterization of the perforatorium, are based on the results of this paper and a culmination of previous work performed in our laboratory. Despite morphological differences, the head of both bovine and rat spermatozoa consists of a nucleus (N, black), acrosome (A, crosshatched), and PT. The acrosome contains an inner acrosomal membrane (IAM) that faces the PT, and an outer acrosomal membrane (OAM) tightly associated with the plasma membrane (PM). The PT is a structurally continuous cytosolic region of the sperm head that encapsulates the entire condensed nucleus, except where the tail implants. (A) A mid-sagittal section of a bovine spermatozoon relative to its three-dimensional structure. The PT of bovine spermatozoa can be divided into the subacrosomal layer (SAL, red) and postacrosomal sheath (PAS, yellow). The SAL occupies the space between the IAM and nuclear envelope, and also includes the outer periacrosomal layer (OPL) along the outer aspect of the equatorial segment (ES) of the acrosome. The PAS extends beyond the SAL in the space between the nuclear envelope and PM, below the acrosome. (B) A mid-sagittal section of a rat spermatozoon, with a superimposed acrosome (light gray) and representative cross-sectional views. In addition to the SAL (with OPL) and PAS, the PT of rat spermatozoa consists of an apical region called the perforatorium (orange). The rat sperm head also contains another apical protrusion called the ventral spur (VS), which is organized into two layers. The acrosomic system of rat differs from bovine in that it contains a ventrally displaced head cap segment (HCS) of which the SAL encapsulates entirely. Note the structural similarity between the caudal cross-sectional images of the rat spermatozoon to the mid-sagittal section of the bovine. M, mitochondria; AX, axoneme. Adapted from Oko and Maravei [4] and Lalli and Clermont [43].

The perforatorium has long been a structure of considerable query with respect to its characterization [30]. Traditionally masked under the identity of the SAL and not regarded as a separate entity of the PT [5, 31, 32], perforatorial biogenesis and molecular composition have not been well elucidated, as compared to the other two regions of the PT. To account for this gap in the literature, the present study sought to provide further insights into the formation and characterization of the perforatorium.

Since the perforatorium and PAS both materialize during the elongation phase of spermiogenesis, we sought to investigate the developmental and compositional similarities and differences between these two regions of the PT. Through the use of cell fractionation, immunoblotting, and immunolocalization techniques, we provide evidence for the distinctiveness of the perforatorium as a region of the PT of falciform spermatozoa. Importantly, we also reveal a compositional similarity between the perforatorium and the PAS, with both regions immunoreactive to proteins previously characterized in spatulate spermatozoa as PAS residents. Our developmental analysis shows that both PAS and perforatorial assembly are fundamentally linked to protein transport on the manchette. While PAS assembly occurs in the wake of manchette descent at the completion of spermatid elongation, perforatorial biogenesis begins prior to the distal migration of the manchette, facilitating the apical translocation of proteins into the perforatorium. Both traditionally PAS-resident (e.g. WBP2NL, core histones) and perforatorial-specific (e.g. PERF15) proteins were found to accumulate in this triangular perforatorial space prior to the condensation of the perforatorium at the conclusion of spermiogenesis. Since the PAS of the PT is one of the first sperm components to solubilize and expel its contents into the ooplasm following fusion of the two gametic membranes, its composition has implications for understanding the events of early fertilization. The compositional similarity between the PAS and perforatorium thus gives insights into the functionality and purpose of the perforatorium in falciform spermatozoa.

Methods and materials

Animals

Experimental procedures involving the use of animals in this study were approved by the University Animal Care Committee (UACC) of Queen's University and complied with the guidelines of the Canadian Council of Animal Care (CCAC). All rat procedures were performed with adult Sprague-Dawley rats purchased from Charles River Laboratories (St. Constant, QC). Porcine spermatozoa were collected at

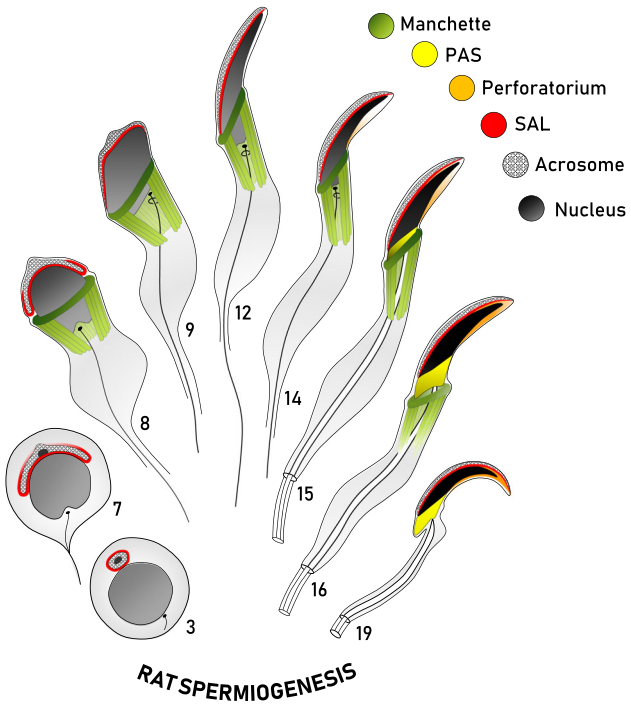

Figure 2. Diagrammatic representation of the formation of the perinuclear theca during rat spermiogenesis. This diagram represents our current working model of the biogenesis of the perinuclear theca (PT) in falciform spermatozoa. Spermatids at representative steps of rat spermiogenesis are depicted in sagittal sections, with some structures drawn to give an appreciation of their three-dimensional range about the nucleus (i.e. manchette, PAS). The manchette (green) emerges at the onset of spermatid elongation and vanishes as the spermatid completes nuclear elongation and condensation, represented by a progressive darkening of the nucleus (gray/black). The spatial and temporal assembly of the three regions of the PT of rat spermatozoa are shown, with the subacrosomal layer (SAL, red) forming early in spermiogenesis concomitant with the acrosome (cross-hatched), and the postacrosomal sheath (PAS, yellow) appearing later as the microtubular manchette migrates distally. Note that the PAS is superimposed on the sagittal drawing to give an appreciation of its range about the caudal aspect of the spermatid nucleus following manchette descent. Similar to PAS formation, the perforatorium (orange) of the PT is also proposed to make use of the manchette for the transport of proteins into this apical compartment. Adapted from Oko [5].

the National Swine Resource and Research Center at the University of Missouri (Columbia, MO). Bovine spermatozoa were obtained from Hilts Butcher Shop Ltd (Norwood, ON), and human sperm samples were donated from the Department of Urology, McGill University Health Center (Montreal, QC).

Antibodies

Primary antibodies

The primary antibodies used in this report included a goat polyclonal anti-GSTO2 antibody (Santa Cruz Biotechnology, Y-12, sc-17943) as formerly validated [25], a rabbit polyclonal anti-WBP2 antibody (ProteinTech, 12030-1-AP) as previously used [33], a rabbit polyclonal affinity-purified anti-histone-H3 antibody (ProteinTech, 17168-1-AP), a mouse monoclonal anti-α-tubulin antibody (Sigma-Aldrich, T6074), a customized rabbit polyclonal affinity-purified anti-PERF15 antibody, and a customized rabbit polyclonal affinity-purified anti-WBP2NL antibody. Immune serum raised in a rabbit against the isolated perforatorial fraction [12] was affinity-purified on the western blot immobilized 15 kDa perforatorial polypeptide (PERF15), as previously described [11]. Affinity-purified WBP2NL antibody was prepared according to a prior method [34].

Primary antibodies for immunoblotting experiments were diluted as follows: PERF15 (1:500), WBP2NL (1:5000), GSTO2 (1:750), WBP2 (1:1000), and histone H3 (1:3000). Immunofluorescence analysis on whole rat spermatozoa made use of the PERF15 (1:20), WBP2NL (1:50), GSTO2 (1:30), WBP2 (1:30), and histone H3 (1:30) antibodies. Immunofluorescence on rat spermatids isolated from the seminiferous tubules was performed with PERF15 (1:20) or WBP2NL serum (1:200), together with α-tubulin (1:500). Immunogold electron microscopy made use of the affinity-purified PERF15 antibody (1:10). Preimmune serum used at the same concentration, or primary antibody together with its respective block, served as control for each experiment performed. Information regarding primary antibodies can also be found in supplementary data (Supplementary Table S1).

Secondary antibodies

Secondary antibodies for immunoblotting included a goat-anti-rabbit IgG HRP (1:30,000; Vector Laboratories, PI-1000) and a rabbit-anti-goat IgG HRP (1:10,000; Santa Cruz, sc-2768). For immunofluorescence, the secondary antibodies used were a donkey-anti-rabbit IgG-CFL 488 (1:100; Santa Cruz Biotechnology, sc-362261) and a donkey-anti-mouse IgG-CFL 647 (1:100; Santa Cruz Biotechnology, sc-362288) along with DAPI (4′,6-diamidino-2-phenylindole, 1:100) for nuclear staining. Immunogold electron microscopy made use of a goat-anti rabbit secondary antibody conjugated to 10 nm colloidal gold particles (1:20; Sigma-Aldrich, Mississauga, ON).

Sperm head separation

Whole rat spermatozoa were sonicated to detach sperm heads from tails [4, 17], and separated from one another in 80% sucrose by ultracentrifugation at 200,000 × *g* for 1 h at 4°C in the presence of a protease inhibitor (0.2 mM phenylmethysulfonyl fluoride), as previously described [35].

Isolation of rat perforatorium

Rat sperm heads, separated from tails, were sonicated until the apical perforatorial tips were detached from the sperm heads, as evidenced by phase contrast microscopy (Zeiss, Model 61458, Germany). Perforatoria were isolated from the remaining sperm heads in a 30/80% discontinuous sucrose gradient by ultracentrifugation at 100,000 × *g* for 15 min at 4°C, as previously described [35]. Rat perforatorial samples were separated by sodium dodecyl sulfate-polyacrylamide gel electrophoresis (SDS-PAGE) and stained with Coomasie Brilliant Blue 250 (Sigma-Aldrich, St. Louis, MO), or used for immunoblotting.

Extraction of the perinuclear theca

Rat sperm heads separated from tails underwent three successive extraction steps consisting of serial incubations in 0.2% Triton-X-100 (1 h), 1 M KCl (1 h), and 100 mM NaOH (overnight), with the latter executed at 4°C with agitation. Following each extraction procedure, the suspension was centrifuged at 2500 × *g* for 10 min, recovering the supernatant and twice washing the pellet by resuspension and centrifugation in phosphate-buffered saline (PBS) before proceeding

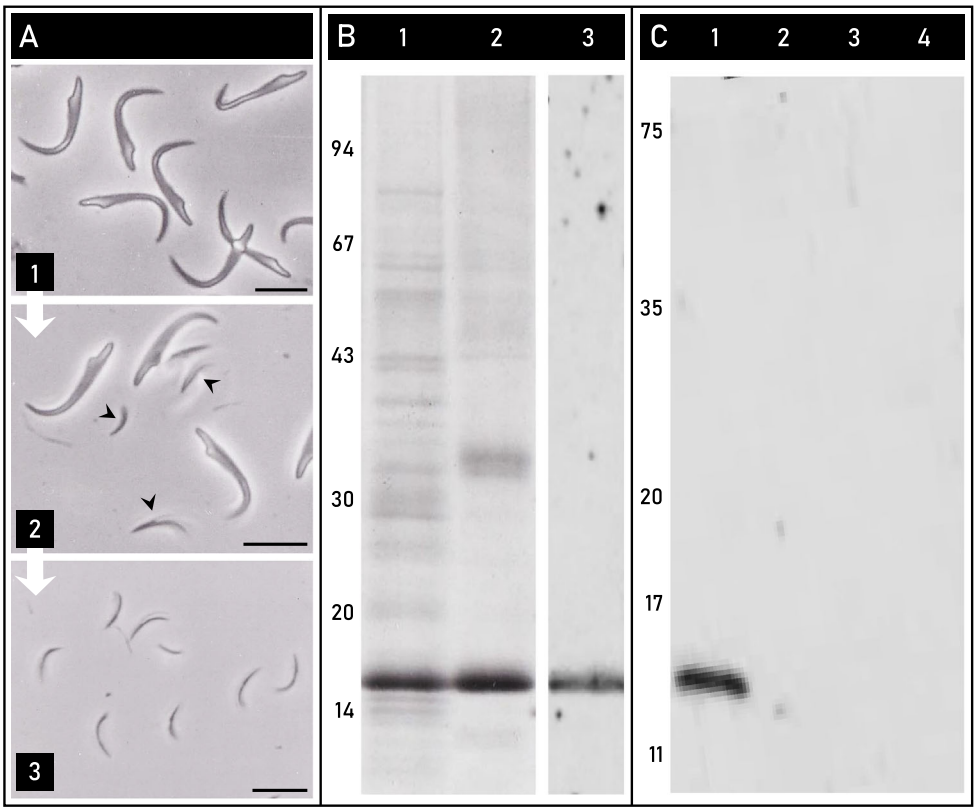

Figure 3. PERF15 is the major protein constituent of the perforatorium. (A) Phase contrast micrographs showing the successive steps involved in the isolation of the perforatorium. Rat sperm heads separated from tails (1) were ultrasonicated to detach the perforatoria (➤) from the nuclei and the remaining PT (2), and then isolated on a sucrose gradient (3). (B) Lanes 1 and 2 represent Coomassie-stained samples of the extracted perinuclear theca (Lane 1) and isolated perforatorium (Lane 2) of rat spermatozoa. In both lanes, the most prominent band is a 15 kDa protein previously identified as PERF15. Lane 3 is a western blot of the isolated rat perforatoria immunolabeled with an affinity-purified anti-PERF15 antibody, showing reactivity to a single band at 15 kDa. (C) Comparison of the presence of PERF15 in falciform and spatulate spermatozoa. Preparative western blots were loaded with rat (lane 1), human (lane 2), bovine (lane 3), and porcine (lane 4) whole sperm samples and probed with an affinity-purified anti-PERF15 antibody. A single immunoreactive band was present in falciform rat spermatozoa, and absent in the other spatulate sperm samples. Bars, 10 μm.

to the next extraction step. Serial incubations served to sequentially solubilize inner acrosomal membrane proteins [35], ionically bound PT proteins [36], and covalently bound PT proteins [9, 26]. Supernatants obtained from the extraction of the PT were separated by SDS-PAGE and stained with Coomassie Brilliant Blue 250 (Sigma-Aldrich, St. Louis, MO).

Gel electrophoresis and immunoblotting

Samples for immunoblotting analysis were solubilized in reducing sample buffer (200 nM Tris pH 6.8, 4% SDS, 0.1% bromophenol blue, 5% β-mercaptoethanol, 40% glycerol), loaded in wells, and run on SDS-PAGE with a BLUeye prestained protein ladder (GeneDirex, Taiwan). Samples consisted of whole spermatozoa (rat, human, bovine, porcine) and isolated rat perforatoria. Electrophoresis-separated proteins were transferred onto activated PVDF (Millipore, Mississauga, ON) or nitrocellulose (Schleicher & Schuell, Dassel, Germany) membranes as previously described [37]. Membrane strips were blocked with 10% skim milk diluted in PBS with 0.05% Tween-20 (PBS-T) prior to primary antibody incubation overnight in 4°C. Blots were washed extensively with PBS-T prior to and following secondary antibody incubation, conjugated with HRP. The membranes were exposed to Western ECL substrate (Bio-Rad Clarity Western ECL Substrate, Mississauga, ON) and developed on an X-ray film (Eastman Kodak Company, Rochester, NY).

Electron microscopy

Tissue preparation

Male rats were anesthetized and the testes and epididymides were fixed by perfusion through the abdominal aorta with either 2.5% glutaraldehyde in 0.1 M cacodylate buffer containing 0.5% $CaCl_2$ for epon embedding or 0.8% glutaraldehyde and 4% paraformaldehyde in 0.1 M phosphate buffer containing 15 mM lysine at pH 7.4 for Lowicryl embedding.

Tissues for Epon 812 embedding were first immersed in respective fixative for 2 h, washed in cold 0.1 M sodium cacodylate buffer (pH 7.2) containing 4% sucrose, and post-fixed for 1 h at 4°C in 1% osmium tetroxide. Dehydration was subsequently carried out in ethanol and propylene oxide before Epon embedding. Tissues for Lowicryl embedding were immersed in respective fixative for 2 h, washed three times in 0.15 M PBS containing 4% sucrose (pH 7.4) at 4°C, and treated with PBS containing 50 mM NH_4Cl for 1 h at 4°C. Tissues were then washed in PBS, dehydrated in graded methanol, and infiltrated and embedded in Lowicryl K4M [38]. Thin sections for immunogold labeling were mounted on formavar coated nickel grids.

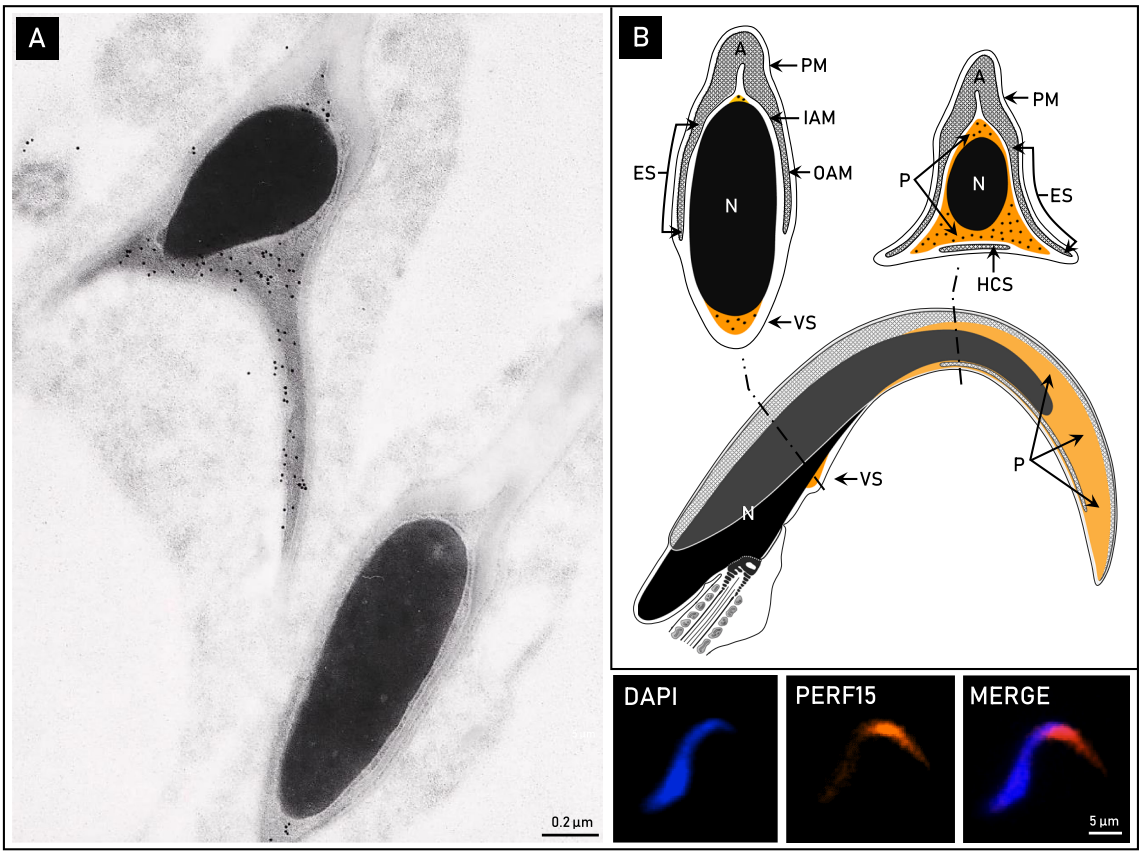

Figure 4. The localization of PERF15 in the perinuclear theca of rat spermatozoa. (A) Immunolocalization with an affinity-purified anti-PERF15 antibody at the ultrastructural and fluorescent levels. Cross-sectional electron micrographs localize PERF15 immunoreactivity to the triangular perforatorium as well as ventral spur (VS). Immunofluorescence appears to dominate the apical perforatorial hook (bottom right). (B) Diagrammatic representation of the pattern of PERF15 labeling in mature rat spermatozoa. A, acrosome; IAM, inner acrosomal membrane; OAM, outer acrosomal membrane; ES, equatorial segment; HCS, displaced head cap segment; PM, plasma membrane; N, nucleus; P, perforatorium.

Immunocytochemistry

Immunocytochemistry on ultrathin sections was executed as previously described [39]. Sections were blocked for 15 min with 10% goat serum in tris-buffered saline, pH 7.4 (TBS) prior to incubation with primary antibody for 1 h. Slides were washed extensively in TBS containing 0.1% Tween-20 (TBS-T) and blocked again with 10% goat serum in TBS. Grids were washed in TBS-T and distilled water before counterstained with uranyl acetate and lead citrate, washed in distilled water and dried. Grids were examined using a Hitachi H-7000 transmission electron microscope.

Fluorescence microscopy

Tissue preparation

Spermatozoa from male rats were taken from the cauda epididymis and vas deferens and submerged into a solution of 0.1 M PBS, pH 7.4. Epididymal spermatozoa were collected by piercing the cauda and allowing the spermatozoa to diffuse into suspension. In a similar manner, spermatozoa from the vas deferens were ejected by applying pressure along the duct to allow the spermatozoa to be expelled. Spermatozoa were isolated by centrifuging the sample at 1000 $\times$ *g* for 5 min and discarding the supernatant. The spermatozoa were resuspended in fixative of 2% formaldehyde (FA) in PBS for 40 min and were used immediately or stored in PBS at 4°C for future use. Testicular cells were collected from the seminiferous tubules by isolating the testes of male rats, removing the tunica albuginea, and expelling the cellular contents of the seminiferous tubules in a solution of PBS. The samples were centrifuged and fixed as described above.

Indirect immunofluorescence

Spermatozoa or testicular cells fixed in 2% FA were combined with KMT buffer (10 mM KCl, 1 mM $MgCl_2$, 10 mM Tris-HCl, pH 7), placed onto poly-L-lysine coated coverslips and left to adhere [40]. The KMT buffer solution was removed and the coverslip-mounted cells were permeabilized in PBS containing 0.1% Triton-X-100 (PBS-Tx) for 40 min at room temperature. Nonspecific binding of antibodies was blocked with 5% normal goat serum (NGS) or 5% bovine serum albumin (BSA) diluted in PBS-Tx for 25 min at room temperature. Primary antibody was left to incubate overnight at 4°C in a humidity chamber. The following day, coverslips were washed with 1% NGS-PBS-Tx or 1% BSA-PBS-Tx prior to a secondary antibody incubation of 40 min at room temperature, away from light. Coverslips were subsequently washed with PBS-Tx, mounted on glass microscope slides with VectaShield mounting media (H-1200, Vector Laboratories, Burlingame, CA) and sealed along the edges with clear nail polish. Slides were stored in darkness at 4°C until visualized by a confocal microscope. Images were captured using a Quorum Wave Effects Spinning Disc Confocal Microscope, and images analysis was performed with MetaMorph Imaging Software.

Results

PERF15 is the major protein constituent of the perforatorium

Rat sperm heads underwent an isolation and fractionation procedure (Figure 3A). Once rat sperm heads (Figure 3A-1) are separated from the tails on a sucrose gradient, they can be used to extract the PT as a whole [7], or ultrasonicated to break the apical perforatorial tips from the sperm nuclei (Figure 3A-2), and isolated on a sucrose gradient (Figure 3A-3) [35]. The protein composition of the extracted PT and isolated tips can be analyzed and compared by PAGE and western blotting.

The extracted PT of rat spermatozoa, separated by PAGE and stained with Coomassie Brilliant Blue 250, revealed an extensive protein-banding pattern (Figure 3B, lane 1), giving appreciation to the complexity of the PT. Among the many bands representing the proteins of the SAL, PAS, and perforatorium, the most prominent was a 15 kDa band previously identified as PERF15 [41]. When the Coomassie-stained PT extract was compared to the isolated perforatorium (Figure 3B, lane 2), the 15 kDa band remained pronounced, indicating its prominence in the perforatorium. Western blots of isolated rat perforatorial tips probed with an affinity-purified anti-PERF15 antibody confirmed the identity of this 15 kDa protein and the specificity of its interaction (Figure 3B, lane 3).

To demonstrate that PERF15 is a distinct component of the perforatorium, and thereby present only in falciform spermatozoa, preparative immunoblots of whole rat spermatozoa (Figure 3C, lane 1) were probed with anti-PERF15 and compared to samples of whole spatulate spermatozoa represented by human, bovine, and porcine spermatozoa (Figure 3C, lanes 2–4). A single band at 15 kDa was present in the lane containing only whole rat spermatozoa and not present in any of the spatulate sperm samples.

Immunogold localization on ultrathin sections of mature rat spermatozoa using an affinity-purified anti-PERF15 antibody exclusively labeled the perforatorium and inner layer of the ventral spur (Figure 4A). Indirect immunofluorescence on whole rat spermatozoa using the same antibody confirmed this reactivity (Figure 4A). Thus, as its major constituent, PERF15 delineates the range of the perforatorium in falciform rat spermatozoa. Immunogold and immunofluorescence controls with preimmune serum were non-reactive.

Compositional similarity between the perforatorium and postacrosomal sheath of the perinuclear theca

Indirect immunofluorescence analysis on mature, whole rat spermatozoa was performed with a collection of antibodies against known PAS proteins identified and characterized in our laboratory. This included WBP2NL, WBP2, GSTO2, and the core histones (represented by histone H3). In all antibodies tested, immunoreactivity was specific to the rounded apical curvature of the perforatorium, as well as obliquely at the opposing end of the sperm head in the PAS (Figure 5A). Whole sperm incubated in preimmune serum or in primary antibody together with its respective peptide block showed no immunoreactivity. To confirm the perforatorial presence of these proteins, isolated perforatorial tips were loaded and probed with each antibody for immunoblotting analysis (Figure 5B). Note that the postacrosomal identities of these proteins have previously been shown in either bovine or murid sperm studies [25, 26, 33, 36].

Preparative western blots of the electrophoretically separated perforatorial fractions were incubated with antibodies against

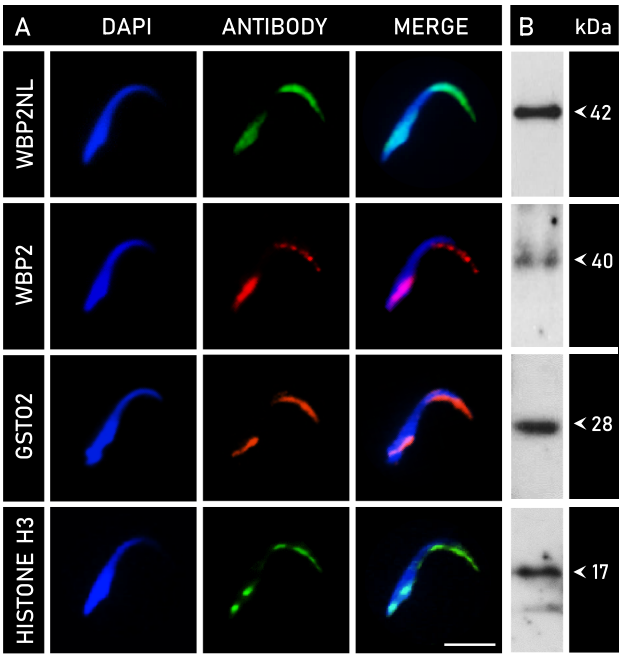

Figure 5. Indirect immunofluorescence analysis of PT proteins in mature rat spermatozoa, with accompanying perforatorial immunoblots. (A) Rows represent the localization pattern observed with indirect immunofluorescence in whole rat sperm with the following antibodies: WBP2NL, WBP2, GSTO2, and histone H3 (representative of core histones). DAPI is indicative of nuclear staining (blue), and antibody labeling is identified accordingly. Immunoreactivity with all antibodies tested was specific to the area of the perforatorium and postacrosomal sheath. The observed perforatorial labeling in falciform spermatozoa is a novelty not observed in spatulate sperm. (B) To confirm the perforatorial identity of these proteins, preparative immunoblots of isolated perforatorial fractions (see Figure 3A-3) were probed with each respective antibody and revealed immunoreactive bands characteristic of each protein. Bars, 10 μm.

WBP2NL, WBP2, GSTO2, and histone H3 (Figure 5B). Anti-WBP2NL labeling was localized to a single band at a molecular mass of approximately 42 kDa. The molecular mass of WBP2NL is species-specific, as shown in previous studies with mouse (38 kDa), porcine (38 kDa), and bovine (32 kDa) spermatozoa [26]. WBP2 labeling was associated with an immunoreactive band at approximately 40 kDa, identical to that demonstrated in mouse spermatozoa [33]. The amount of sonication required to isolate the perforatorium has been shown to decrease the content of WBP2 in the PT, thereby accounting for a weaker than expected reactivity [33]. Immunoreactivity for GSTO2 in rat perforatorial samples migrated to a band at 28 kDa, corresponding to its most prominent isoform [25]. Anti-histone H3 labeling in the perforatorium was strongest at approximately 17 kDa, but displayed a second, faint band at around 14 kDa, which was indicative of breakdown product, to which histone H3 is very prone [36].

Developmental origin and assembly of the perforatorium

To explore the developmental homogeny between the PAS and perforatorium, spermatids at various steps of spermiogenesis were analyzed with indirect immunofluorescence to trace the formation of the developing PT (Figure 6). Spermatids extracted from the seminiferous tubules of rat were double-labeled with an

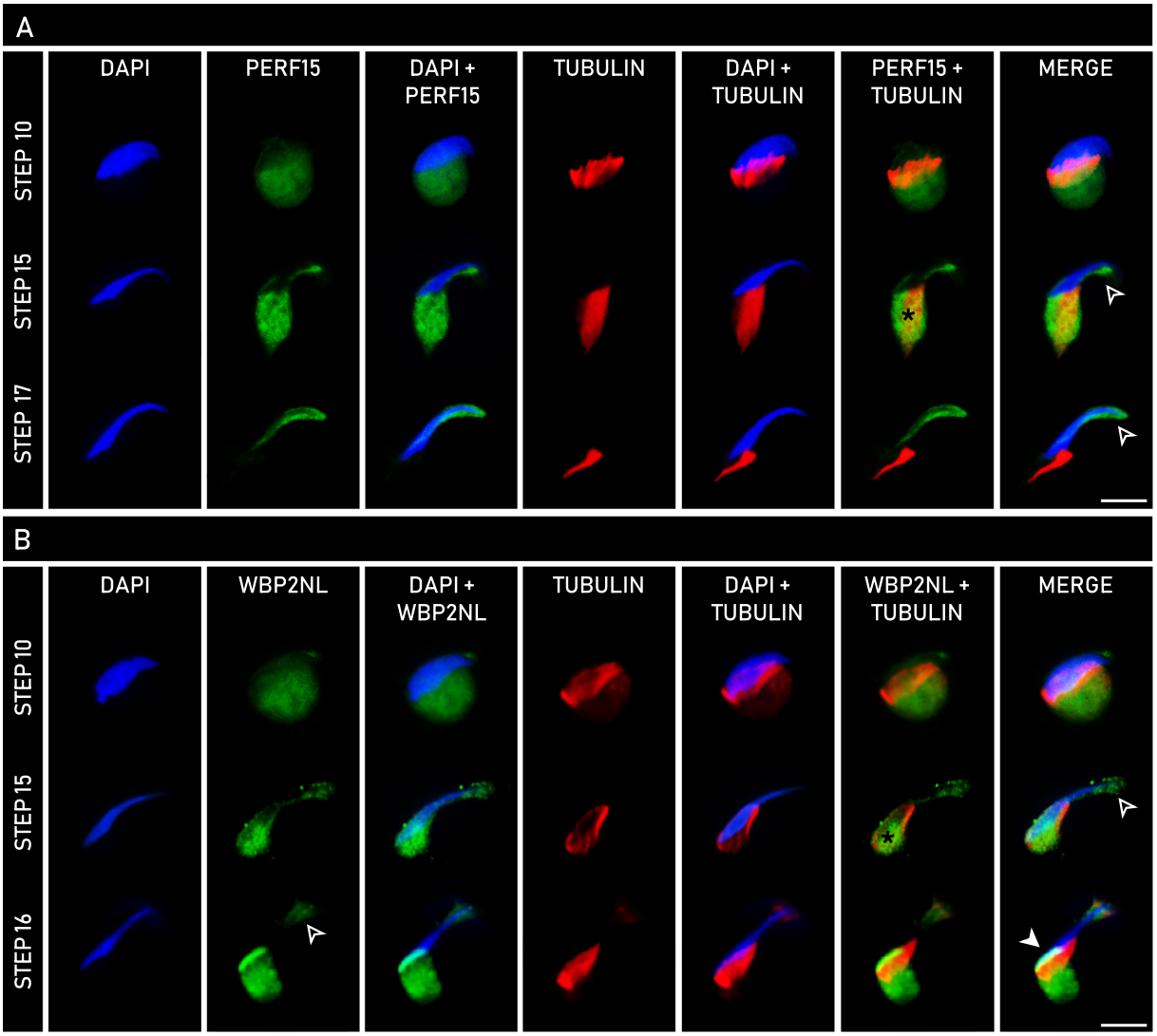

Figure 6. Comparative developmental expression of PERF15 (A) and WBP2NL (B) with α-tubulin in spermatids throughout rat spermiogenesis using indirect immunofluorescence. Columns represent the type of analysis performed, with DAPI (blue) indicative of nuclear staining, α-tubulin (red) representative of manchette microtubules, and PERF15 (A, green) or WBP2NL (B, green) showing their respective expression. In both PERF15 and WBP2NL panels, labeling is seen in the distal cytoplasmic lobe and co-localized with α-tubulin on the manchette (*). Note that PERF15 only localizes to the perforatorial region (➢), while WBP2NL localizes to both the perforatorium (➢) and PAS (➤). Bars, 10 μm.

anti-α-tubulin antibody and an anti-WBP2NL or anti-PERF15 antibody. WBP2NL, a known PAS-resident and a newly identified perforatorial occupant, was used as a model to demonstrate the origin and assembly of both the PAS and perforatorium during spermiogenesis, whereas PERF15 was used to showcase the assembly of just the latter.

Labeling of both WBP2NL and PERF15 was detected in the distal cytoplasmic lobe of newly elongating spermatids (Figure 6A and B, step 10) as a circular mass beneath the manchette. Anti-α-tubulin labeling, representative of the microtubules of the manchette, encased the caudal spermatid head, extending its range from the nucleus to the cytoplasmic lobe. As spermatids progressed further into the elongation phase of spermiogenesis (Figure 6A and B, step 15), labeling of both WBP2NL and PERF15 co-localized with α-tubulin, indicating protein detection on the manchette. In addition to the manchette, WBP2NL and PERF15 reactivity was seen along the ventral edge of the spermatid head and at its most apical tip (Figure 6A and B, step 15). Labeling became more prominent at the apex of the spermatid head in later stage spermatids labeled with PERF15 (Figure 6A, step 17). WBP2NL maintained apical reactivity in spermatids at a comparable step of spermiogenesis (Figure 6B, step 16). As the manchette migrated downwards at the conclusion of spermatid elongation, WBP2NL reacted in the area once occupied by the microtubules in the basal region of the sperm head as an oblique line indicative of the PAS (Figure 6B, step 16). The distal migration of the manchette was associated with a decrease in its girth as it came off the nucleus. PERF15 labeling was void in this distal region, but immunoreactivity continued to increase in intensity apically in the perforatorium (Figure 6A, step 17). Similar steps of spermiogenesis were shown for both PERF15 and WBP2NL for ease of comparison. Spermatids incubated in preimmune serum served as negative controls.

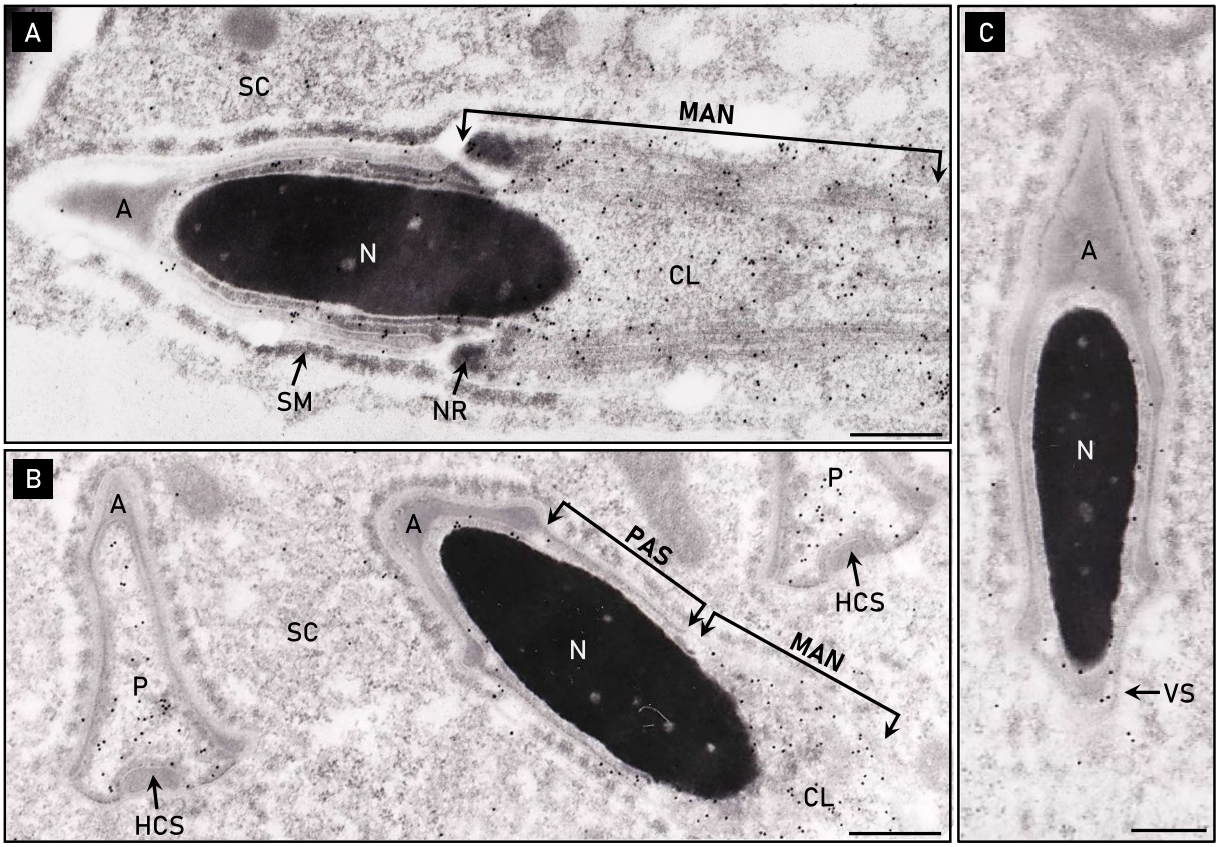

Figure 7. Electron micrographs of rat spermatids immunolabeled with anti-PERF15 antibody. (A) PERF15 is predominantly localized to the distal cytoplasmic lobe (CL) and microtubular manchette (MAN) of a step 13 rat spermatid. (B) Accumulation of PERF15 in a pre-condensed, electron-lucent perforatorium (P), but distinctly void in the forming postacrosomal sheath (PAS) below the acrosome (A) of a step 15–16 spermatid. Labeling also occurs over the distally migrating manchette. Note the PAS is not present prior to manchette descent (see Figure 7A), but appears only after the manchette has migrated down the spermatid nucleus (N). (C) PERF15 labeling in the area of the ventral spur (VS) of a step 16 spermatid. HCS, displaced head cap segment; NR, nuclear ring; SM, Sertoli cell mantel; SC, Sertoli cell cytoplasm. Bars, 0.2 μm.

Electron micrographs of elongating rat spermatid sections immunolabeled with an anti-PERF15 antibody provided further insights into the formation of the perforatorium. Consistent with indirect immunofluorescence data, elongating spermatids localized PERF15 to the caudal manchette and cytoplasmic lobe distal to the nucleus of a step 13 rat spermatid (Figure 7A). Manchette microtubules are tightly packed between the plasma membrane and nuclear envelope, making the manchette the likely route to transport PT proteins to the spermatid head region. Following manchette descent of a step 15–16 rat spermatid, the newly formed PAS region of the PT was void of any anti-PERF15 labeling (Figure 7B). Cross-sectional electron micrographs of the triangular perforatorial compartment prior to its condensation revealed an accumulation of anti-PERF15 immunoreactivity amid the borders of the acrosomic system (Figure 7B). The acrosome covers the superior and lateral aspects of the perforatorium, while exposing its base to a continuous channel of cytosol along the ventral underbelly of the spermatid head. The ventral surface lacks a bordering acrosome, but contains the displaced head cap segment, a product of acrosomal fission during spermiogenesis. In addition to the perforatorium, PERF15 labeling was also localized to the area of the ventral spur in a step 16 spermatid (Figure 7C). Spermatids incubated in preimmune serum lacked immunogold labeling.

The change in position of the manchette relative to the step of rat spermiogenesis was further demonstrated with electron micrographs of Epon embedded step 14 and step 15–16 rat spermatids (Supplementary Figure S1). The manchette was seen to circumnavigate the nucleus below the acrosome of an elongating spermatid, extending its microtubules from the nuclear ring to the cytoplasmic lobe. The manchette then migrated distally from its circumnuclear position during steps 15–16 of rat spermiogenesis, narrowing its girth about the nucleus as it descended. Insights obtained from these electron micrographs assisted in developing the diagrammatic illustrations of the manchette in the present study.

Discussion

The present study sought to review and analyze the regional formation of the PT of falciform spermatozoa during spermiogenesis, with a focus on elucidating the biogenesis and characterization of the perforatorium. Our findings demonstrate that the perforatorium forms during the latter half of spermiogenesis via a similar process of developmental assembly to the PAS. In support of the developmental homogeny between the perforatorium and PAS, we report a compositional likeness between these two cytosolic PT compartments, while also acknowledging a regional distinction that differentiates

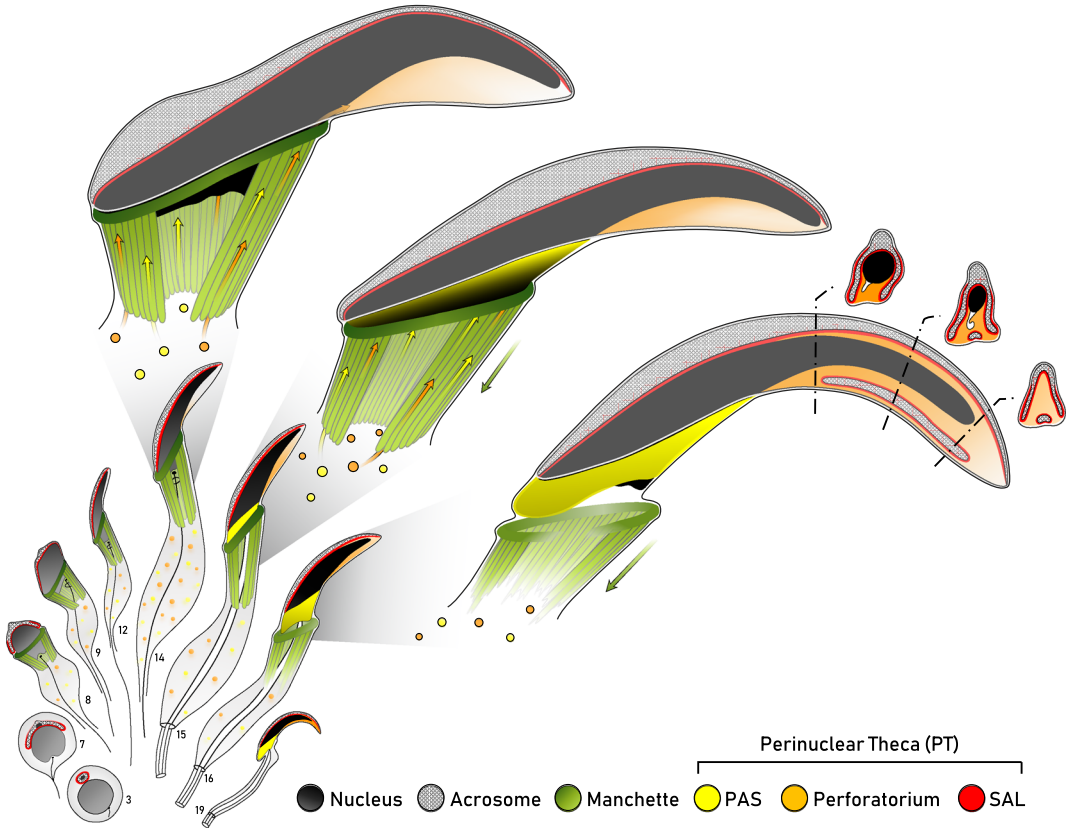

Figure 8. Diagrammatic summary of the developmental steps proposed in the formation of the perforatorium and postacrosomal sheath (PAS) of the perinuclear theca (PT) of rat spermatozoa. Spermatids progressing through spermiogenesis are shown in sagittal sections, although some structures have been superimposed to give an appreciation of their three-dimensional architecture. Attention is paid to spermatids of step 14–16 to demonstrate the proposed assembly of the perforatorium and PAS of falciform spermatozoa. Where appropriate, representative cross-sectional views of the spermatid head provide an alternative perspective of PT biogenesis. Perforatorial-bound proteins (orange) synthesized in the distal cytoplasmic lobe of elongating spermatids migrate upwards on the manchette and pass ventrally along the spermatid head into the perforatorium. The ventral void in acrosomal material, seen in cross-sectional views, permits the passage of proteins, leading to the progressive infiltration of material in the perforatorium. Similarly, PAS-bound proteins (yellow) also make use of the manchette for the storage and transport of proteins prior to their deposition in the PAS upon manchette descent. The manchette, PAS, and acrosome are drawn to give an appreciation of their three-dimensional range in the spermatid head. Note that the subacrosomal layer (SAL, red) forms early in spermiogenesis, synchronously with the acrosome and remains adherent to the inner acrosomal membrane as the sperm head markedly expands in the creation of the perforatorium. Adapted from Lalli and Clermont [43].

them as separate entities of the PT. We found that previously characterized PAS proteins, deemed essential for fertilization in spatulate spermatozoa, also reside in the murid sperm perforatorium, giving insights into the functional significance of the perforatorium in falciform spermatozoa.

The developmental steps involved in the assembly of the perforatorium and PAS are summarized in Figure 8. Perforatorial biogenesis was deduced by tracing the expression of the most prominent perforatorial constituent, PERF15, throughout spermiogenesis using a combination of immunocytochemical techniques. Our analysis indicates that the perforatorium, like the PAS, is dependent on the manchette for the transport and deposition of proteins into the apical PT compartment during the elongation phase of spermiogenesis. After being translocated by the manchette, we propose PT proteins diffuse apically along the ventral surface of the spermatid head into the forming triangular perforatorial space, in addition to being deposited in the PAS upon manchette descent.

PAS- and perforatorial-bound proteins were initially detected in the distal cytoplasmic lobe of elongating spermatids, indicating that they are synthesized near the nascent tail compartment of the spermatid. PERF15 mRNA has previously been shown to be first translated during meiotic prophase of germ cell development. Its product later becomes highly expressed in the distal cytoplasm of elongating spermatids [42], in agreement with our analysis. Likewise, WBP2NL mRNA translation begins at the end of round spermatid development before reaching peak translation in the distal cytoplasm of elongating spermatids [21]. These developmental origins are likely a common characteristic feature of all PT proteins of the PAS and perforatorium.

From the cytoplasmic lobe, the microtubule-based caudal manchette appears to be the only transport mechanism for conveying PAS and perforatorial proteins to the spermatid head. Facilitated by intramanchette transport, proteins are mobilized along the microtubules of the manchette to their subcellular destination [23, 24]. The role of the manchette in PAS formation has been well documented [1, 17, 21, 22, 25, 33]. As the manchette migrates distally at the completion of spermatid elongation, PAS-bound proteins stored on the manchette are translocated into the space created by its descent [21, 22, 25, 33]. The microtubules of the manchette are tightly sandwiched between the plasma membrane and nuclear envelope,

making its descent a requirement for PAS assembly. In addition to PAS biogenesis, we also demonstrate the novel role of the manchette in perforatorial formation.

The apical expansion into which the perforatorium materializes markedly increases during steps 15–16 of rat spermiogenesis into a triangular cytoplasmic space of low density [43] (see Figure 8, steps 15–16). This distinct morphological expansion unique to the head of most murids coincides with protein localization on the manchette, and the accumulation of perforatorial-bound proteins in the forming perforatorium. The means by which perforatorial proteins accumulate during this period of spermatid development is thereby likely to be facilitated by the manchette. Since PAS formation is dependent upon the distal migration of the manchette as spermatid elongation and nuclear condensation concludes, the deposition of perforatorial proteins most likely precedes its descent. This indeed appears to be the case for PERF15 and WBP2NL, as the apical region of step 15 spermatids are already immunoreactive for these two proteins before manchette descent. Although the perforatorium amasses its constituents at this time of spermatid development, it is only during the final two steps of spermiogenesis when the perforatorium condenses into its definitive, electron-dense structure [12].

The proposed method of perforatorial assembly is further reflected in the structural organization of the head of falciform spermatozoa. The acrosomic system of falciform spermatozoa forms a triangular crest over the dorsal and lateral edges of the sperm head, while the ventral border is void of acrosomal material except for a vestige of acrosome termed the displaced head cap segment (see Figure 8, step 16 cross sections). The displaced head cap segment is a product of acrosomal fission during spermiogenesis that detaches from one of the two lateral sides of the acrosome and migrates to the base of the perforatorium [43]. Interruption of the acrosome ventrally creates a continuous cytosolic channel along the concave surface of the spermatid head that can facilitate the passage of proteins rostrally into the perforatorium. This is in contrast to spatulate spermatozoa, whose acrosomic system circumnavigates the entire sperm head, preventing apical protein movement and the formation of a perforatorium. With this in mind, it would thereby be unlikely for perforatorial protein passage in falciform spermatozoa to occur dorsally or laterally, as these regions are occluded by the acrosome and SAL. Also, likely facilitating the ventral movement of these proteins is the angular orientation of the manchette in falciform spermatozoa, which reaches further ventrally (Supplementary Figure S1).

In support for the developmental homogeny between the PAS and perforatorium, fluorescent immunolocalization indicates the perforatorium is compositionally similar to the PAS. Several known PT proteins, including WBP2NL, WBP2, GSTO2, and the core histones (represented by histone H3) were localized to both the PAS and perforatorium of rat spermatozoa. This pattern of labeling is also conserved in mouse [25, 33]. In spatulate spermatozoa (i.e. human, bovine, porcine), however, which lack a perforatorium, the immunoreactivity of most of the aforementioned proteins (WBP2NL, GSTO2, core histones) remains exclusive to the PAS (Supplementary Figure S2). The additional localization of these proteins to the perforatorium points to the functional significance of the perforatorium as an extension of the PAS. Perhaps during perforatorial deposition, PERF15 intermixes with the PAS proteins to ensure their even distribution and then later is involved in the condensation of this fluid-filled cavity. Proteins localized to the PAS have been implicated in early fertilization and zygotic development. Most notably, WBP2NL and its ortholog, WBP2, are candidate oocyte-activating factors [26, 27, 33], while the sperm-borne, PT-localized GSTO2 and core histones have been implicated in sperm nuclear remodeling events early in zygotic development [1, 25, 36]. As the sperm head solubilizes apically, protein redundancy in the perforatorium could be advantageous in providing an equal distribution of these proteins in the sickle-shaped sperm head of murids. This could ensure the prolonged and continual delivery of paternal factors into the oocyte during the crucial early stages of fertilization.

Authors' Contributions

RO, NP, and LH designed the project with guidance from PS. LH, NP, and RW performed the experiments, with the technical support of WX. The manuscript was written by NP with contributions from LH, RO, and PS. The diagrammatic illustrations were created by NP.

Supplementary data

Supplementary data are available at *BIOLRE* online.

Supplementary Table S1. Antibody table.

Supplementary Figure S1. Electron micrographs of elongating rat spermatids showing the change in manchette position during spermatid elongation. (A) The microtubular manchette (MAN) surrounds the nucleus (N) of a step 14 rat spermatid. The microtubules extend from the nuclear ring below the acrosome to the distal cytoplasmic lobe. The angular nature of the manchette allows it to reach higher along the ventral surface of the nucleus. (B) The distal migration of the manchette of a step 15–16 rat spermatid. The descent of the manchette is associated with a narrowing of its girth about the nucleus. Note the change in position of the annulus (AN), which lowers following manchette descent. NR, nuclear ring; MS, mitochondrial sheath; AX, axoneme. Bars, 0.5 μm.

Supplementary Figure S2. Immunolocalization of WBP2NL, GSTO2 and core histones in the postacrosomal sheath of spatulate spermatozoa.

References

1. Oko R, Sutovsky P. Biogenesis of sperm perinuclear theca and its role in sperm functional competence and fertilization. *Am J Anat* 2009; **83**:419–434.
2. Sutovsky P, Manandhar G, Wu A, Oko R. Interactions of sperm perinuclear theca with the oocyte: implications for oocyte activation, antipolyspermy defense, and assisted reproduction. *Microsc Res Tech* 2003; **61**:362–378.
3. Sutovsky P, Oko R, Hewitson L, Schatten G. The removal of the sperm perinuclear theca and its association with the bovine oocyte surface during fertilization. *Dev Biol* 1997; **188**:75–84.
4. Oko R, Maravei D. Protein composition of the perinuclear theca of bull spermatozoa. *Biol Reprod* 1994; **50**:1000–1014.
5. Oko R. Developmental expression and possible role of perinuclear theca proteins in mammalian spermatozoa. *Reprod Fertil Dev* 1995; **7**:777–797.
6. Oko R, Moussakova L, Clermont Y. Regional differences in composition of the perforatorium and outer periacrosomal layer of the rat spermatozoon as revealed by immunocytochemistry. *Am J Anat* 1990; **188**:64–73.
7. Mountjoy JR, Xu W, McLeod D, Hyndman D, Oko R. RAB2A: a major subacrosomal protein of bovine spermatozoa implicated in acrosomal biogenesis. *Biol Reprod* 2008; **79**:223–232.
8. Tran MH, Aul RB, Xu W, van der Hoorn FA, Oko R. Involvement of classical bipartite/karyopherin nuclear import pathway components in acrosomal trafficking and assembly during bovine and murid spermiogenesis. *Biol Reprod* 2012; **86**:84.
9. Aul RB, Oko RJ. The major subacrosomal occupant of bull spermatozoa is a novel histone H2B variant associated with the forming acrosome during spermiogenesis. *Dev Biol* 2002; **242**:376–387.

10. Courtens JL, Courot M, Fléchon JE. The perinuclear substance of boar, bull, ram and rabbit spermatozoa. *J Ultrastruct Res* 1976; **57**:54–64.
11. Oko R, Clermont Y. Origin and distribution of perforatorial proteins during spermatogenesis of the rat: an immunocytochemical study. *Anat Rec* 1991; **230**:489–501.
12. Oko R, Clermont Y. Isolation, structure and protein composition of the perforatorium of rat spermatozoa. *Biol Reprod* 1988; **39**:673–87.
13. Breed W. Evolution of the spermatozoon in Australasian rodents. *Aust J Zool* 1997; **45**:459–478.
14. Breed WG. Sperm head structure in the hydromyinae (rodentia:Muridae): a further evolutionary development of the subacrosomal space in mammals. *Gamete Res* 1984; **10**:31–44.
15. Breed WG, Idriss D, Oko RJ. Protein composition of the ventral processes on the sperm head of Australian hydromyine rodents. *Biol Reprod* 2000; **63**:629–634.
16. Flaherty SP, Breed WG. The sperm head of the plains mouse, Pseudomys australis: ultrastructure and effects of chemical treatments. *Gamete Res* 1983; **8**:231–244.
17. Oko R, Maravei D. Distribution and possible role of perinuclear theca proteins during bovine spermiogenesis. *Microsc Res Tech* 1995; **32**:520–532.
18. O'Donnell L, O'Bryan MK. Microtubules and spermatogenesis. *Semin Cell Devl Biol* 2014; **30**:45–54.
19. Barth AD, Oko RJ. Normal bovine spermatogenesis and sperm maturation. in *Abnormal Morphology of Bovine Spermatozoa*. Ames: Iowa State University Press; 1989:19–88.
20. Longo FJ, Cook S. Formation of the perinuclear theca in spermatozoa of diverse mammalian species: relationship of the manchette and multiple band polypeptides. *Mol Reprod Dev* 1991; **28**:380–393.
21. Wu ATH, Sutovsky P, Xu W, van der Spoel AC, Platt FM, Oko R. The postacrosomal assembly of sperm head protein, PAWP, is independent of acrosome formation and dependent on microtubular manchette transport. *Dev Biol* 2007; **312**:471–483.
22. Tovich PR, Sutovsky P, Oko RJ. Novel aspect of perinuclear theca assembly revealed by immunolocalization of non-nuclear somatic histones during bovine spermiogenesis. *Biol Reprod* 2004; **71**:1182–1194.
23. Kierszenbaum AL. Intramanchette transport (IMT): Managing the making of the spermatid head, centrosome, and tail. *Mol Reprod Dev* 2002; **63**:1–4.
24. Kierszenbaum AL, Gil M, Rivkin E, Tres LL. Ran, a GTP-binding protein involved in nucleocytoplasmic transport and microtubule nucleation, relocates from the manchette to the centrosome region during rat spermiogenesis. *Mol Reprod Dev* 2002; **63**:131–140.
25. Hamilton LE, Acteau G, Xu W, Sutovsky P, Oko R. The developmental origin and compartmentalization of glutathione-s-transferase omega 2 isoforms in the perinuclear theca of eutherian spermatozoa. *Biol Reprod* 2017; **97**:612–621.
26. Wu ATH, Sutovsky P, Manandhar G, Xu W, Katayama M, Day BN, Park K-W, Yi Y-J, Xi YW, Prather RS, Oko R. PAWP, a sperm-specific WW domain-binding protein, promotes meiotic resumption and pronuclear development during fertilization. *J Biol Chem* 2007; **282**:12164–12175.
27. Aarabi M, Balakier H, Bashar S, Moskovtsev SI, Sutovsky P, Librach CL, Oko R. Sperm-derived WW domain-binding protein, PAWP, elicits calcium oscillations and oocyte activation in humans and mice. *FASEB J* 2014; **28**:4434–4440.
28. Young C, Grasa P, Coward K, Davis LC, Parrington J. Phospholipase C zeta undergoes dynamic changes in its pattern of localization in sperm during capacitation and the acrosome reaction. *Fertil Steril* 2009; **91**:2230–2242.
29. Saunders CM, Larman MG, Parrington J, Cox LJ, Royse J, Blayney LM, Swann K, Lai FA. PLC zeta: a sperm-specific trigger of Ca(2+) oscillations in eggs and embryo development. *Development* 2002; **129**:3533–3544.
30. Olson GE, Hamilton DW, Fawcett DW. Isolation and characterization of the perforatorium of rat spermatozoa. *Reproduction* 1976; **47**:293–297.
31. Müjica A, Navarro-García F, Hernández-González EO, De Lourdes Juárez-Mosqueda M. Perinuclear theca during spermatozoa maturation leading to fertilization. *Microsc Res Tech* 2003; **61**:76–87.
32. Lin Y-W, Hsu T-H, Yen PH. Mouse sperm acquire a new structure on the apical hook during epididymal maturation. *Asian J Androl* 2013; **15**:523–528.
33. Hamilton LE, Suzuki J, Acteau G, Shi M, Xu W, Meinsohn M-C, Sutovsky P, Oko R. WBP2 shares a common location in mouse spermatozoa with WBP2NL/PAWP and like its descendent is a candidate mouse oocyte activating factor. *Biol Reprod* 2018; **99**:1171–1183.
34. Aarabi M, Balakier H, Bashar S, Moskovtsev SI, Sutovsky P, Librach CL, Oko R. Sperm content of postacrosomal WW binding protein is related to fertilization outcomes in patients undergoing assisted reproductive technology. *Fertil Steril* 2014; **102**:440–447.
35. Yu Y, Xu W, Yi Y-J, Sutovsky P, Oko R. The extracellular protein coat of the inner acrosomal membrane is involved in zona pellucida binding and penetration during fertilization: characterization of its most prominent polypeptide (IAM38). *Dev Biol* 2006; **290**:32–43.
36. Tovich PR, Oko RJ. Somatic histones are components of the perinuclear theca in bovine spermatozoa. *J Biol Chem* 2003; **278**:32431–32438.
37. Towbin H, Staehelin T, Gordon J. Electrophoretic transfer of proteins from polyacrylamide gels to nitrocellulose sheets: procedure and some applications. *Proc Natl Acad Sci USA* 1979; **76**:4350–4354.
38. Grant DS, Kleinman HK, Leblond CP, Inoue S, Chung AE, Martin GR. The basement-membrane-like matrix of the mouse EHS tumor: II. Immunohistochemical quantitation of six of its components. *Am J Anat* 1985; **174**:387–398.
39. Oko R, Jando V, Wagner CL, Kistler WS, Hermo LS. Chromatin reorganization in rat spermatids during the disappearance of testis-specific histone, H1t, and the appearance of transition proteins TP1 and TP2. *Biol Reprod* 1996; **54**:1141–1157.
40. Sutovsky P. Visualization of sperm accessory structures in the mammalian spermatids, spermatozoa, and zygotes by immunofluorescence, confocal, and immunoelectron microscopy. In: Schatten H (ed.), *Germ Cell Protocols: Volume 1: Sperm and Oocyte Analysis*. Totowa, NJ: Humana Press; 2004:59–77.
41. Oko R, Morales CR. A novel testicular protein, with sequence similarities to a family of lipid binding proteins, is a major component of the rat sperm perinuclear theca. *Dev Biol* 1994; **166**:235–245.
42. Korley R, Pouresmaeili F, Oko R. Analysis of the protein composition of the mouse sperm perinuclear theca and characterization of its major protein constituent. *Biol Reprod* 1997; **57**:1426–1432.
43. Lalli M, Clermont Y. Structural changes of the head components of the rat spermatid during late spermiogenesis. *Am J Anat* 1981; **160**:419–434.